The University of Maine
DigitalCommons@UMaine

2-1-2009

Chevkinite-Group Minerals from Granulite-Facies Metamorphic Rocks and Associated Pegmatites of East Antarctica and South India

H. E. Belkin

R. Macdonald

Edward S. Grew
University of Maine - Main, esgrew@maine.edu

Follow this and additional works at: https://digitalcommons.library.umaine.edu/ers_facpub

Part of the Earth Sciences Commons

Repository Citation
Belkin, H. E.; Macdonald, R.; and Grew, Edward S., "Chevkinite-Group Minerals from Granulite-Facies Metamorphic Rocks and Associated Pegmatites of East Antarctica and South India" (2009). *Earth Science Faculty Scholarship*. 23.
https://digitalcommons.library.umaine.edu/ers_facpub/23

This Article is brought to you for free and open access by DigitalCommons@UMaine. It has been accepted for inclusion in Earth Science Faculty Scholarship by an authorized administrator of DigitalCommons@UMaine. For more information, please contact um.library.technical.services@maine.edu.

Mineralogical Magazine, February 2009, Vol. 73(1), pp. 149–164

Chevkinite-group minerals from granulite-facies metamorphic rocks and associated pegmatites of East Antarctica and South India

H. E. BELKIN[1,*], R. MACDONALD[2,3] AND E. S. GREW[4]

[1] U.S. Geological Survey, 956 National Center, Reston, VA 20192, USA
[2] IGMiP Faculty of Geology, University of Warsaw, Al. Żwirki i Wigury 93, 02-089 Warsaw, Poland
[3] Environment Centre, Lancaster University, Lancaster LA1 4YQ, UK
[4] Department of Earth Sciences, University of Maine, 5790 Bryand Center, Orono, ME 04469, USA

[*Received 17 December 2008; Accepted 22 April 2009*]

ABSTRACT

Electron microprobe data are presented for chevkinite-group minerals from granulite-facies rocks and associated pegmatites of the Napier Complex and Mawson Station charnockite in East Antarctica and from the Eastern Ghats, South India. Their compositions conform to the general formula for this group, *viz.* $A_4BC_2D_2Si_4O_{22}$ where, in the analysed specimens A = (rare-earth elements (*REE*), Ca, Y, Th), B = Fe^{2+}, Mg, C = (Al, Mg, Ti, Fe^{2+}, Fe^{3+}, Zr) and D = Ti and plot within the perrierite field of the total Fe (as FeO) (wt.%) *vs*. CaO (wt.%) discriminator diagram of Macdonald and Belkin (2002). In contrast to most chevkinite-group minerals, the *A* site shows unusual enrichment in the *MREE* and *HREE* relative to the *LREE* and Ca. In one sample from the Napier Complex, Y is the dominant cation among the total *REE* + Y in the *A* site, the first reported case of Y-dominance in the chevkinite group. The minerals include the most Al-rich yet reported in the chevkinite group ($\leqslant$9.15 wt.% Al_2O_3), sufficient to fill the *C* site in two samples. Conversely, the amount of Ti in these samples does not fill the *D* site, and, thus, some of the Al could be making up the deficiency at *D*, a situation not previously reported in the chevkinite group. Fe abundances are low, requiring Mg to occupy up to 45% of the *B* site. The chevkinite-group minerals analysed originated from three distinct parageneses: (1) pegmatites containing hornblende and orthopyroxene or garnet; (2) orthopyroxene-bearing gneiss and granulite; (3) highly aluminous paragneisses in which the associated minerals are relatively magnesian or aluminous. Chevkinite-group minerals from the first two parageneses have relatively high FeO content and low MgO and Al_2O_3 contents; their compositions plot in the field for mafic and intermediate igneous rocks. In contrast, chevkinite-group minerals from the third paragenesis are notably more aluminous and have greater Mg/Fe ratios.

KEYWORDS: chevkinite-group, perrierite, Antarctica, Eastern Ghats, India.

Introduction

THE most abundant members of the chevkinite group (Table 1), chevkinite-(Ce) and perrierite-(Ce), are found in igneous rocks ranging from gabbros to peralkaline granites, and in fenites, ore deposits, granulite-facies gneisses and meta-carbonates. In terms of crystal structure, these two minerals are dimorphs (e.g. Bonatti and Gottardi, 1966; Sokolova *et al*., 2004), but chemical data show that they are compositionally distinct; chevkinites tend to have greater total Fe (FeO* = total iron as Fe^{2+}) and Ce_2O_3 and smaller CaO and Al_2O_3 than perrierites (e.g. van Bergen, 1984; Macdonald and Belkin, 2002).

In a review of compositional variation in minerals of the chevkinite group, Macdonald

---

* E-mail: hbelkin@usgs.gov
DOI: 10.1180/minmag.2009.073.1.149

© 2009 The Mineralogical Society

TABLE 1. Possible end-members in the chevkinite group, $A_4BC_2D_2Si_4O_{22}$.

End-member	Chevkinite subgroup	Perrierite subgroup
$Ce_4Fe^{2+}(Fe^{3+}_2)Ti_2Si_4O_{22}$	**Chevkinite-(Ce), Maoniupingite-(Ce)**	Perrierite-(Ce) in part
$Ce_4Fe^{2+}(Fe^{2+}Ti)Ti_2Si_4O_{22}$	**Dingdaohengite-(Ce)**	Perrierite-(Ce) in part
$Ca_4Ti(Ti_2)Ti_2Si_4O_{22}$	In maoniupingite-(Ce)	Ca-analogue of matsubaraite
$Sr_4Ti(Ti_2)Ti_2Si_4O_{22}$		**Matsubaraite**
$Sr_4Zr(Ti_2)Ti_2Si_4O_{22}$		**Rengeite**
$Ca_4Zr(Ti_2)Ti_2Si_4O_{22}$		Ca-analogue of rengeite
$Ce_4Zr(Fe^{2+}_2)Ti_2Si_4O_{22}$		In strontio-chevkinite
$Ce_4Mg(Cr^{3+}_2)Ti_2Si_4O_{22}$	**Polyakovite-(Ce)**	
$Ce_4Mg(Al_2)Ti_2Si_4O_{22}$		Mg, Al analogue of perrierite-(Ce)
$Ce_4Fe^{2+}(Al_2)Ti_2Si_4O_{22}$		Al analogue of perrierite-(Ce)

Names accepted by the CNMNC IMA are in bold. Subgroups implied by the dimorphism of chevkinite-(Ce) and perrierite-(Ce) (Sokolova *et al.*, 2004).

and Belkin (2002) suggested that further compositional variants, or even new species, might be found in parageneses unusual for the group, such as high-grade metamorphic rocks. They also called for further analyses of perrierite, which is less-well documented than chevkinite. Compared to chevkinite, relatively few compositions plotting in the perrierite field of Macdonald and Belkin (2002) have been reported since 2002, e.g. Zr-rich perrierite from Peru (Carlier and Lorand, 2008) and a Sc-bearing perrierite from Inner Mongolia, China (Shimazaki *et al.*, 2008). In this paper, we present electron microprobe analyses of chevkinite-group minerals in granulites and associated pegmatites from East Antarctica and South India, with the specific aim of furthering our knowledge of the compositional range of minerals in the group.

The results also brought to light nomenclature problems in the chevkinite group. New species have been approved on an *ad hoc* basis with little attempt to choose which crystallographic sites should serve as criteria for distinguishing species, as has been done for other complex mineral groups, most recently the sapphirine group (Grew *et al.*, 2008). In view of the potentially chaotic situation in chevkinite-group nomenclature and for want of a better term, we will refer to our minerals simply as 'chevkinite-group minerals'.

Source of the samples

Beginning with the reports by Atrashenok *et al.* (1967) and Kamenev (1972) of a 'metasomatic chevkinite' from a fissure in charnockite of the Archaean Napier Complex, Enderby Land, Antarctica (Fig. 1), minerals of the chevkinite group have been reported from several localities in Antarctica, including Napier granulite-facies rocks (Grew and Manton, 1979*a*; Hokada, 2007), the Mawson Station charnockite (Grew and Manton, 1979*b*), and a partially melted sapphirine granulite xenolith in norite in the Vestfold Hills, ~600 km east of Mawson Station (Harley, 1994). Grew and Manton (1986) also reported perrierite from a sapphirine-bearing migmatite in the Eastern Ghats Province, South India. Only the Vestfold Hills and Mt. Riiser-Larsen (Napier Complex) samples were completely analysed; the others were used for isotopic dating for which only Th, U and Pb contents are needed. The present paper reports data on the chevkinite-group minerals studied by Grew and Manton, together with a few samples from nearby localities, i.e. five samples from four localities (Mt. Charles, Mt. Cronus, Zircon Point, Fyfe Hills) in the Napier Complex, Enderby Land, East Antarctica, one from the Mawson Station charnockite, MacRobertson Land, East Antarctica, and four (3080P, R, T, U) from Anakapalle in the Eastern Ghats Province of South India (Fig. 1).

Geological background

Rocks exposed along the periphery of East Antarctica between 45ºE and 65ºE belong to the Archaean Napier Complex and Proterozoic Rayner Complex, both granulite-facies complexes with long histories extending from ~3800 to

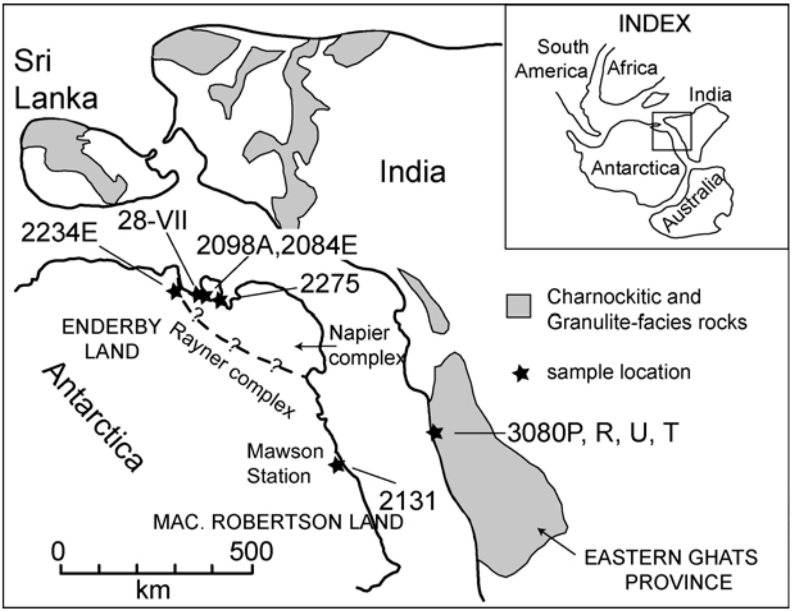

FIG. 1. Locality map; details of the individual samples can be found in the text (simplified from Grew and Manton, 1986).

~500 Ma (e.g. Grew and Manton, 1979*a*; Sheraton *et al*., 1987; Halpin *et al*., 2005). Four of our samples (28-VII, 2084E, 2234E, 2275) and that studied by Hokada (2007) are granulites from the southwestern part of the complex, where metamorphic temperatures are estimated to have reached 1070ºC and pressures of 7−10 kbar (e.g. Harley, 1998, 2008). Sample 2098A is from a pegmatite vein at Mt. Charles, also in the southwestern part of the complex. The vein was emplaced at ~2500 Ma and conditions of crystallization were earlier estimated to be as high as 1000−1100ºC at 9−11 kbar (Grew *et al*., 2000). Although the vein probably crystallized at very high temperatures, the 1000−1100ºC estimate might be too high because veins of this generation were emplaced after the peak of ultrahigh-temperature metamorphism (Grew *et al*., 2006). Sample 2131 is from a pegmatite dated at 850 Ma (Grew and Manton, 1979*b*) that cuts one of the Mawson charnockites, a group of Rayner Complex hypersthene adamellites, quartz monzodiorites and granodiorites emplaced soon after peak metamorphism and dated at 985−954 Ma (e.g. Sheraton, 1982; Young and Black, 1991; Young *et al*., 1997; Halpin *et al*., 2005).

The Eastern Ghats Province probably represents an extension of the late Proterozoic Rayner Complex into India (Grew and Manton, 1979*a*, 1986). Our samples are sapphirine-bearing migmatites from near Anakapalle, possibly an Archaean or early Proterozoic rock (age $\geqslant$2000 Ma), reworked during late Proterozoic metamorphism at 1000 Ma (Grew and Manton, 1986). Like the Napier Complex, the Eastern Ghats belt is an ultrahigh-temperature complex, metamorphosed under conditions of 7−10 kbar, 900 to >1000ºC (e.g. Sengupta *et al*., 1999; Bose *et al*., 2000; Sarkar *et al*., 2003).

Sample descriptions

2234E

Sample 2234 is a garnet-biotite-sillimanite quartzo-feldspathic granulite from the Napier Complex at Zircon Point in Casey Bay (Grew *et al*., 2006). Sapphirine occurs only as inclusions in garnet. The chevkinite-group mineral is optically isotropic (metamict) and forms an aggregate several mm across with quartz and garnet adjacent to a garnet porphyroblast (Fig. 2*a*). The mineral encloses sillimanite, and is also found enclosed in garnet and sapphirine, textural relationships suggesting that the mineral crystallized over a time interval including the metamorphic peak. One subhedral 2 mm crystal has been analysed.

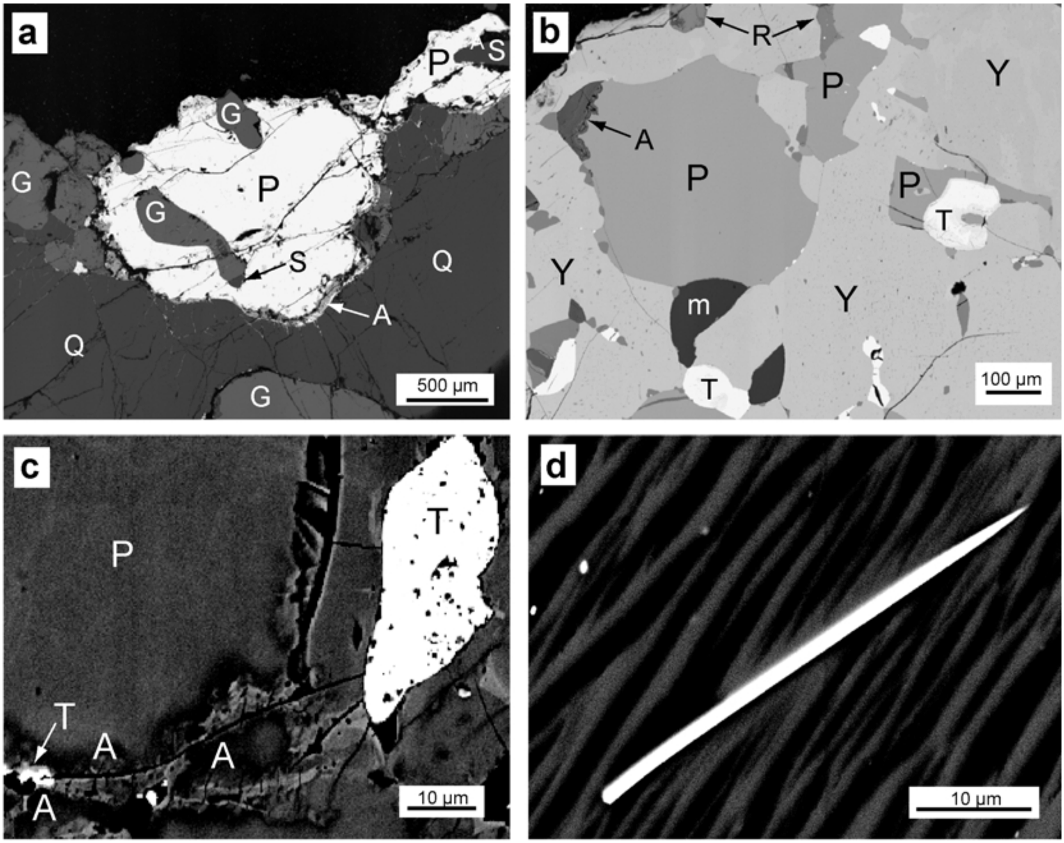

FIG. 2. SEM-BSE images of varying contrasts showing the textural settings and mineral associations of the Antarctic and Indian chevkinite-group minerals. (*a*) Millimetre-size grain of a chevkinite-group mineral (P) from sample 2234E along the edge of a thin section with inclusions of garnet (G) and sillimanite (S) in a quartz (Q) and garnet (G) assemblage. An irregular altered (A) rim around the chevkinite-group mineral is somewhat depleted in *REE*. (*b*) Anhedral grains of a chevkinite-group mineral (P) from sample 2275 enclosed by yttrium titanoniobate (Y) with biotite (m), rutile (R) and altered and unaltered thorite (T). The chevkinite-group mineral is altered (A) along fractures. (*c*) A portion of a large grain of a chevkinite-group mineral (P) from sample 2098A that has been somewhat altered (A) along fractures in which thorite (T) has precipitated. (*d*) Acicular chevkinite-group mineral in mesoperthite from sample 3080T.

2275 – Mt. Cronus, Napier Complex

This is a light-grey, fine-grained, orthopyroxene-garnet-biotite-bearing, quartzo-feldspathic gneiss (Asami *et al.*, 1998, 2002). Plagioclase, containing abundant antiperthitic lamellae, is the dominant phase. Other phases include rutile, an ore mineral and zircon. A red-brown to olive, optically isotropic (metamict) yttrium titanoniobate, possibly polycrase, occurs as rounded to ellipsoidal aggregates 0.2–0.7 mm across, commonly enclosed in garnet. The chevkinite-group mineral forms 100–500 µm, light-brown, rounded, metamict grains enclosed in the polycrase (?), which also includes thorite (Fig. 2*b*); these relationships suggest that the mineral crystallized at close to metamorphic peak conditions. Some outer portions of the mineral are altered; our analyses come from the higher $\bar{Z}$ ($\bar{Z}$ = mean atomic number), unaltered area in six grains.

2098A

The chevkinite-group mineral in 2098A forms an optically isotropic (metamict) mass ~5 cm across in a pegmatite cutting orthopyroxene-bearing quartzo-feldspathic gneisses of the

Napier Complex at Mt. Charles (Grew and Manton, 1979*a*; Grew, 1998; Grew *et al*., 2000). Essential constituents of the pegmatite are quartz, perthite, antiperthite, orthopyroxene, hornblende mantled by orthopyroxene-plagioclase symplectite, and zircon; the chevkinite-group mineral appears also to be a primary pegmatite phase; it contains thorite and altered thorite in slightly-altered areas defined by fractures (Fig. 2*c*); both slightly altered and unaltered areas were analysed. This mineral was identified as 'perrierite' by Grew and Manton (1979*a*) using X-ray diffraction (XRD) of metamict material reconstituted by heating at 700–1000ºC in air or in a reducing atmosphere, an approach suggested by Lima-de-Faria (1962).

2084E – Napier Complex

This specimen is from a quartzo-feldspathic gneiss containing minor orthopyroxene and trace garnet, biotite, zircon, allanite and a chevkinite-group mineral from a second locality on Mt. Charles. Allanite and the mineral, generally found adjacent to orthopyroxene, are optically active. Acicular 250 µm and elongate 200 µm grains were analysed.

28-VII

This is a medium-grained, quartzo-feldspathic granulite from the Napier Complex at the Fyfe Hills (DePaolo *et al*., 1982). Whole-rock analysis gives a metaluminous composition, with 0.2 normative diopside. The dominant phases reported by these authors are plagioclase (66% modal), K-feldspar (15%), quartz (12%) and orthopyroxene (5%), with 1% each opaque and apatite and trace amounts of hornblende, biotite, chlorite, zircon, monazite and a chevkinite-group mineral. The last forms rare, brown, isotropic, metamict grains. A 60 µm slightly altered grain was analysed.

2131

This pegmatite from Mawson Station, MacRobertson Land, Antarctica contains quartz, feldspar, garnet, apatite, hornblende, biotite, zircon and a chevkinite-group mineral (Grew and Manton, 1979*b*). The last is metamict, dark brown and translucent only in thin slivers. Four 10–40 µm grains in allanite were analysed.

Textures in 2084E, 28-VII, and 2131 do not preclude a high-temperature origin for the chevkinite-group mineral in these samples, but they are not sufficiently definitive for us to draw conclusions about the timing of crystallization of this mineral.

3080P, R, U and T

Samples 3080P, R and U are from the same quarry, north of Anakapalle (Grew, 1982), as is sample 3080T described by Grew and Manton (1986). Like 3080T, samples 3080P, R and U are feldspathic layers or diffuse, cross-cutting pegmatitic veinlets, both forms typical of migmatitic sapphirine granulites at Anakapalle. These rocks are dominated by mesoperthitic feldspar up to several centimetres across, with subordinate quartz and orthopyroxene, and local garnet, biotite, sillimanite, sapphirine, zircon, monazite and a chevkinite-group mineral. The last forms pleochroic grains up to 0.1 mm long in garnet and in association with sillimanite, sapphirine, biotite and rutile and also occurs as uncommon acicular crystals in mesoperthite (Fig. 2*d*). It also forms nearly isotropic (metamict) grains several millimetres across. Textures suggest that the chevkinite-group mineral crystallized coevally with sapphirine and garnet (Grew and Manton, 1986).

3080P – anhedral, subhedral and rounded grains, from 10 to 200 µm in size – analysed.

3080R – anhedral grains ranging in size from 30 µm to 2 mm – analysed.

3080U – sub- to anhedral grains ranging in size from 10 to 70 µm – analysed.

3080T – subhedral grains and euhedral blades, from 10 to 70 µm – analysed.

Analytical methods

Quantitative analyses of major and minor elements were made using the equipment and techniques described by Macdonald and Belkin (2002). The relative accuracy is 1–2% for oxide concentrations, >1 wt.% and 5–10% for oxide concentrations <1 wt.%. Minor element detection limits are as follows: Pb = 800 ppm; Gd, Dy, Sm and Pr = 400 ppm; Hf and Ta = 300 ppm; Sr, Nb, Nd, Tb, and Yb = 200 ppm; and all other elements at ~100 ppm. Sodium and U were not detected in any sample.

Unit-cell formulae were calculated on the basis of 22 oxygens, and all Fe was assumed to be Fe^{2+}. Following the method used by Parodi *et al.* (1994), Song *et al.* (1999) and Macdonald and Belkin (2002), cations were allocated to sites as follows: (1) the rare-earth elements (*REE*), Ca, Sr, Na, Ba, K, Pb and Th enter the *A* site; (2) the *B* site is filled to 1 in the order Fe^{2+} ± Mn ± Mg; (3) Ti fills the *D* site to a maximum of 2; (4) the tetrahedral sites are filled firstly by Si and, if necessary, made to 4 with Al ± Ti. The remaining Fe^{2+}, Ti, Al, Mn and Mg enter the *C* site, along with Zr, Nb and Ta.

Representative analyses are given in Table 2; the full data set of 122 analyses is deposited with the Principal Editor of *Mineralogical Magazine* and is available on-line at: www.minersoc.org/pages/e_journals/dep_mat_mm.html.

In most of the newly analysed samples (Table 2 and Supplementary Table), total oxides vary between 98% and 101%. However, in some grains within samples 3080P and 2084E, analytical totals are between 96 and 98 wt.%. We suggest that these grains may have been secondarily hydrated, as has been suspected for metamict samples from Virginia and Mali by Macdonald and Belkin (2002). The cation sum varies from 12.9−13.2, close to the theoretical value of 13. The sum of cations in the *A* site (theoretically 4) is in the range 3.8 to 4.0 and in the *C* site 1.9 to 2.1 (theoretically 2). We believe, therefore, that our analyses are essentially complete with Fe^{3+} much subordinate to Fe^{2+} and that and that the minerals are close to being stoichiometric.

Haggerty and Mariano (1983) suggested that the β angle is the most reliable way of distinguishing chevkinite (100º) from perrierite (113º). However, Macdonald and Belkin (2002) were unable to detect any compositional differences between chevkinites and perrierites classified using β angles and those classified on the basis of powder XRD for which the full chemical data sets had not been published and/or structurally refined. Grew and Manton (1979*a*) identified Antarctic phases as perrierite on this basis. The Antarctic and Eastern Ghats minerals also plot in the perrierite field in the discriminator diagram of Macdonald and Belkin (2002) (Fig. 3).

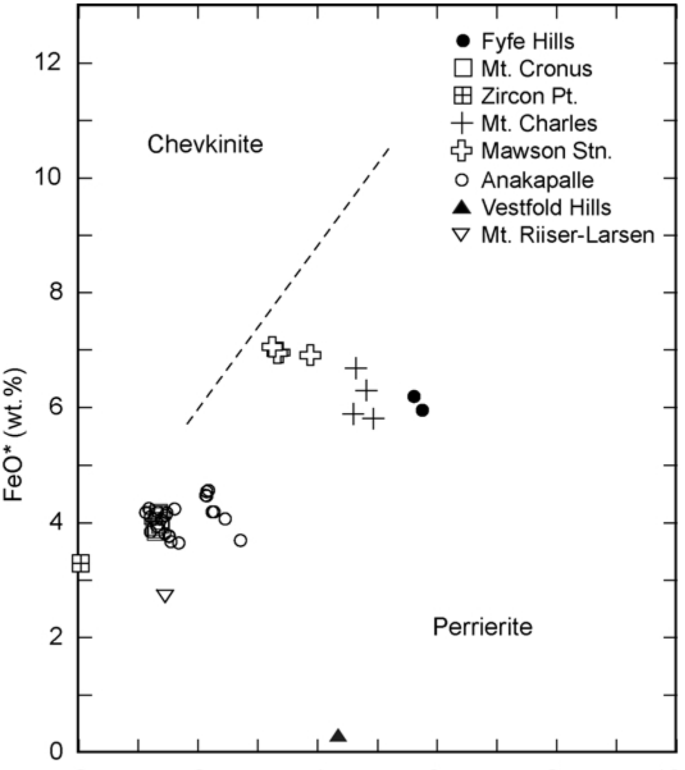

FIG. 3. Antarctic and Eastern Ghats chevkinite-group minerals plotted on the CaO-FeO* discriminator of Macdonald and Belkin (2002).

F-*K*α-Ce-*M*ζ interference

Fluorine concentrations were determined in the studied perrierites by the electron microprobe routine described in Macdonald and Belkin (2002). Examination of the data revealed a high correlation between Ce and F abundance when Ce_2O_3 >10 wt.%. This suggested a relationship that did not have a crystallochemical basis but which may have been the result of peak interference. Following up on the suggestion by Martin Yates (pers. comm., 2005), we investigated the interference between F-*K*α (λ = 18.3199 Å) and Ce-*M*ζ (λ=18.3499 Å). Ce-*M*ζ intensity relative to the strongest Ce-*M* line, Ce-*M*α, is calculated to be I = 1 to 10,000 (Johnson and White, 1970), i.e. within the background of F-*K*α measured with a W/Si LDE1 diffraction crystal (2*d* = 80 Å) supplied by JEOL USA, Inc for a mineral with the high Ce content characteristic of perrierite. Using the LDE1 crystal with a P10 flow detector, we measured Ce-*M*ζ intensity relative to Ce-*M*α intensity using F-free synthetic CeO_2 and Ce phosphate and Ce-*M*α/Ce-*M*ζ ranged from 4 to 5. These much lower intensity ratios are consistent with studies of the *M* spectrum that have found the *M*ζ relative intensities to differ greatly from their ideal values (Wendt and Christ, 1985; Crisp, 1991). Thus, we conclude that the F values reported in chevkinite and perrierite determined by electron microprobe measurement are probably in error and represent Ce-*M*ζ interference. We suggest that a systematic F study of chevkinite-group minerals be undertaken using SIMS or LA-ICP-MS methods.

Composition of perrierites

The A site

Total cations in the *A* site range between 3.83 and 4.02. The main variation in the Antarctic and Indian chevkinite-group minerals, in common with other members of this group, is the substitution of the *REE* for Ca (Fig. 4). The mineral in sample 2234E (Zircon Point) is unusually Ca-poor compared to perrierite (see also Fig. 3). Macdonald and Belkin (2002) noted that, in chevkinite-group minerals, (La+Ce+Ca) normally contribute >75% of the *A* site, i.e. the *REE* abundances in the group normally are dominated by the *LREE*, e.g. $(\Sigma\text{La}-\text{Sm})/(\Sigma_{\text{total}}REE)$ = 0.97. However, (La+Ce+Ca) exceeds 75% in only ~10% of our analyses, the others being between 50 and 75%, with one value at 27%. In ~70% of our analyses, $(\Sigma\text{La}-\text{Sm})/(\Sigma_{\text{total}}REE)$ <0.97, in one case (sample 2275) being as low as 0.57. The

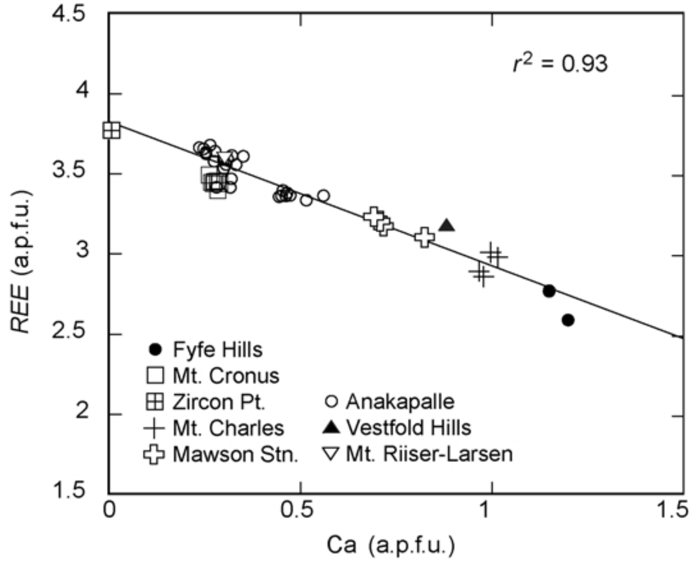

FIG. 4. Relationship between the *REE* and Ca contents of the Antarctic and Eastern Ghats chevkinite-group minerals. Thorium was not included in this plot. The regression line (slope = −0.9) is coincident with that determined by Macdonald and Belkin (2002) for chevkinite and perrierite globally; however, the studied data set has a higher regression coefficient reflecting more consistent analytical methods.

TABLE 2. New chemical analyses and structural formulae of chevkinite-group minerals from Antarctica and India.

Locality	Antarctica							Eastern Ghats, India					
Spec.no.	2131	2275	2098A	2084E	2084E	28-VII	2234E	3080U	3080U	3080R	3080R	3080P	3080P
n	2	3	15	3	3	3	8	1	1	6	2	1	3
Nb_2O_5	0.55	0.09	0.63	0.08	0.04	0.08	1.88	b.d.	b.d.	b.d.	b.d.	0.04	b.d.
Ta_2O_5	0.04	b.d.	b.d.	b.d.	b.d.	0.04	0.15	0.05	b.d.	b.d.	b.d.	b.d.	b.d.
SiO_2	21.11	21.18	21.72	21.59	21.81	21.36	20.55	21.49	20.94	20.94	21.45	20.99	20.77
TiO_2	15.57	12.09	15.86	16.67	17.17	16.63	9.52	14.79	14.20	14.86	15.08	13.92	14.91
ZrO_2	0.19	b.d.	0.29	0.35	0.37	0.66	0.04	b.d.	0.03	0.08	0.03	b.d.	0.10
ThO_2	2.13	4.13	3.20	0.56	0.10	4.60	1.75	0.11	0.42	2.69	1.61	2.92	2.16
Al_2O_3	4.95	8.76	5.09	5.69	5.77	5.57	9.04	6.80	7.19	6.65	7.23	7.36	6.36
La_2O_3	9.57	2.17	8.18	9.24	9.36	9.85	9.81	9.79	5.91	6.72	6.86	5.26	9.82
Ce_2O_3	21.21	8.11	18.49	19.20	19.10	18.19	24.91	26.69	22.79	23.09	19.95	18.15	23.44
Pr_2O_3	2.20	1.54	1.84	1.81	1.95	1.56	2.82	2.62	3.08	3.00	2.25	2.56	2.51
Nd_2O_3	7.45	9.84	5.93	6.65	6.55	5.38	10.78	8.33	12.97	12.27	9.00	11.10	9.53
Sm_2O_3	0.90	5.40	0.95	0.77	0.56	0.45	1.12	1.04	2.14	1.30	1.15	1.82	1.09
Eu_2O_3	–	0.49	–	–	–	–	–	–	–	–	–	–	–
Gd_2O_3	0.53	5.79	0.94	0.84	0.82	0.39	0.53	0.93	1.91	0.52	1.55	2.08	0.34
Tb_2O_3	b.d.	0.60	0.07	0.09	0.05	b.d.	b.d.	b.d.	0.11	b.d.	0.11	0.13	b.d.
Dy_2O_3	0.23	2.76	0.54	0.42	0.44	0.08	0.10	0.18	0.50	0.04	0.96	1.08	b.d.
Ho_2O_3	–	0.23	–	–	–	–	–	–	–	–	–	–	–
Yb_2O_3	b.d.	0.09	0.15	0.16	0.13	b.d.	0.05	b.d.	b.d.	b.d.	0.02	0.07	0.03
Y_2O_3	1.18	8.47	2.66	2.48	2.47	0.41	0.84	0.51	1.06	0.11	4.25	4.42	0.12
FeO*	6.96	4.04	6.69	6.30	5.81	5.97	3.30	4.19	3.86	4.49	3.71	3.78	4.56
MnO	0.05	b.d.	0.19	0.02	b.d.	b.d.	b.d.	b.d.	b.d.	b.d.	b.d.	b.d.	b.d.
MgO	0.72	1.69	0.93	0.76	0.72	0.93	2.27	2.24	2.15	1.96	1.78	2.06	1.89
CaO	3.36	1.37	4.64	4.80	4.92	5.73	0.03	1.45	1.19	2.13	2.69	1.50	2.12
PbO	b.d.	0.55	0.27	b.d.	b.d.	0.46	0.22	b.d.	b.d.	b.d.	b.d.	0.08	b.d.
K_2O	b.d.	b.d.	b.d.	b.d.	b.d.	0.03	b.d.	0.14	0.04	b.d.	b.d.	0.02	b.d.
Total	98.90	99.39	99.26	98.48	98.14	98.37	99.71	101.35	100.49	100.85	99.68	99.34	99.75

Formulae based on 22 oxygens													
Th	0.096	0.185	0.141	0.025	0.004	0.203	0.080	0.005	0.019	0.120	0.070	0.131	0.097
La	0.702	0.158	0.585	0.658	0.663	0.706	0.726	0.698	0.429	0.485	0.488	0.382	0.716
Ce	1.545	0.586	1.312	1.356	1.343	1.295	1.832	1.888	1.642	1.657	1.408	1.309	1.698
Pr	0.160	0.111	0.130	0.127	0.137	0.110	0.206	0.184	0.221	0.214	0.158	0.184	0.181
Nd	0.529	0.694	0.411	0.458	0.449	0.374	0.773	0.575	0.912	0.859	0.620	0.781	0.673
Sm	0.062	0.367	0.063	0.051	0.037	0.030	0.078	0.069	0.145	0.087	0.077	0.124	0.074
Eu	–	0.033	–	–	–	–	–	–	–	–	–	–	–
Gd	0.035	0.379	0.061	0.054	0.052	0.025	0.036	0.060	0.125	0.034	0.099	0.136	0.022
Tb	0.000	0.039	0.005	0.006	0.003	0.000	0.001	0.001	0.007	0.001	0.007	0.009	0.000
Dy	0.015	0.176	0.034	0.026	0.027	0.005	0.007	0.011	0.032	0.002	0.060	0.068	0.000
Ho	–	0.014	–	–	–	–	–	–	–	–	–	–	–
Yb	0.000	0.006	0.009	0.010	0.007	0.000	0.003	0.000	0.000	0.000	0.001	0.004	0.002
Y	0.125	0.889	0.274	0.254	0.252	0.042	0.090	0.052	0.111	0.012	0.436	0.463	0.013
Ca	0.716	0.289	0.962	0.993	1.011	1.193	0.005	0.300	0.251	0.446	0.556	0.317	0.449
Pb	0.000	0.029	0.000	0.000	0.000	0.024	0.012	0.000	0.000	0.000	0.000	0.004	0.000
K	0.000	0.000	0.000	0.000	0.000	0.006	0.000	0.035	0.009	0.000	0.000	0.005	0.000
Sum *A*	3.985	3.955	3.987	4.018	3.985	4.013	3.849	3.878	3.903	3.917	3.980	3.917	3.925
Fe^{2+}	1.000	0.666	1.000	1.000	0.932	0.971	0.555	0.677	0.635	0.736	0.598	0.623	0.754
Mn	0.000	0.000	0.000	0.000	0.001	0.001	0.000	0.000	0.000	0.000	0.001	0.000	0.000
Mg	0.000	0.334	0.000	0.000	0.067	0.028	0.445	0.323	0.365	0.264	0.401	0.377	0.246
Sum *B*	1.000	1.000	1.000	1.000	1.000	1.000	1.000	1.000	1.000	1.000	1.000	1.000	1.000
Fe^{2+}	0.158	0.000	0.083	0.017	0.000	0.000	0.000	0.000	0.000	0.000	0.000	0.000	0.000
Mn	0.009	0.000	0.032	0.003	0.000	0.000	0.000	0.000	0.000	0.000	0.000	0.000	0.000
Mg	0.215	0.163	0.269	0.218	0.140	0.241	0.235	0.322	0.265	0.309	0.109	0.228	0.310
Ti	0.324	0.000	0.306	0.412	0.473	0.426	0.000	0.143	0.096	0.183	0.181	0.057	0.212
Al	1.157	2.033	1.159	1.292	1.303	1.272	2.134	1.545	1.664	1.532	1.639	1.705	1.478
Zr	0.018	0.000	0.028	0.034	0.035	0.063	0.004	0.000	0.003	0.007	0.002	0.000	0.010
Nb	0.059	0.009	0.066	0.008	0.004	0.009	0.205	0.000	0.000	0.000	0.000	0.004	0.002
Ta	0.002	0.000	0.001	0.000	0.000	0.002	0.008	0.003	0.000	0.001	0.000	0.000	0.000
Sum *C*	1.942	2.205	1.944	1.984	1.955	2.013	2.586	2.013	2.028	2.032	1.931	1.994	2.012
Ti (*D*)	2.000	1.788	2.000	2.000	2.000	2.000	1.434	2.000	2.000	2.000	2.000	2.000	2.000
Si	4.186	4.162	4.195	4.152	4.172	4.138	4.114	4.138	4.105	4.089	4.122	4.120	4.093
Σcations	13.113	13.110	13.126	13.154	13.112	13.164	12.983	13.029	13.036	13.038	13.033	13.031	13.030

Total iron reported as FeO*.
b.d. = below detection.
– = not determined.

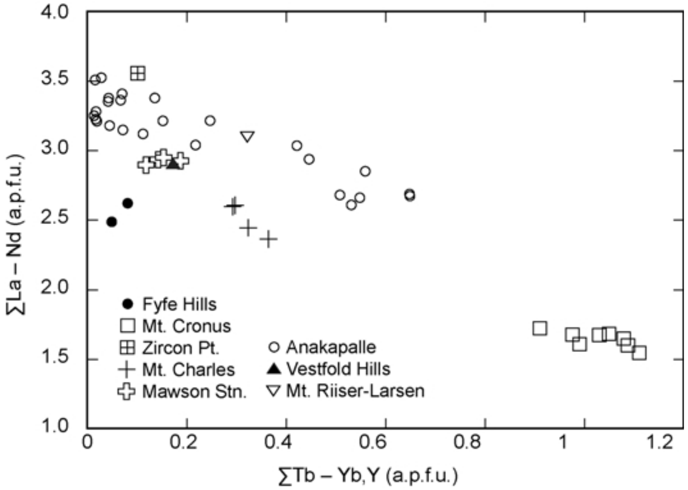

FIG. 5. Relationship between *LREE* (ΣLa–Nd) and *HREE* (ΣTb–Yb, Y) showing a reciprocal trend. Sample 2275 from Mt. Cronus is the most *LREE* depleted and *HREE* enriched and the Anakapalle samples (3080 R, U, P, T) show the greatest variability.

reason for these differences is that compared to perrierite, many of the Antarctic and Eastern Ghats minerals are relatively rich in *HREE* and Y, especially Y (up to 8.47 wt.% Y_2O_3, sample 2275, Mt. Cronus). Indeed, Y is the dominant cation among the total *REE* + Y in the *A* site in this sample, the first record of a Y-dominant mineral in the chevkinite group.

In contrast to the considerable variation in *LREE* abundances reported by Macdonald and Belkin (2002) in chevkinite-group minerals from a wide range of parageneses, the studied minerals show a more limited range; La/Ce (atomic) ranges from 0.23 to 0.56 and La/Nd ranges from 0.20 to 1.92. La/Sm ranges from 2.41 to 47.1, excluding sample 2275. Sample 2275 (Mt. Cronus) is, on average, the most depleted in *LREE* and enriched in *MREE*, as well as Y and *HREE* (Figs 5, 6). Figure 5 also shows that Anakapalle samples have the greatest range in *LREE*/*HREE*. *LREE* enrichment dominates the chondrite-normalized rare-earth pattern (Fig. 6) and the slope is similar to chevkinite (Macdonald and Belkin, 2002) but with higher *MREE*. The scatter shown in *HREE* (Fig. 6) is in part analytical and argues for further study by the LA-ICP-MS technique.

Apart from Ca and the *REE*, the only other notable element in the *A* site is Th, which can reach up to 0.28 a.p.f.u. Strontium was only detected in about 15 analyses at a level just at or above the detection limit.

The B site

The *B* site in chevkinite and perrierite is invariably filled entirely by Fe^{2+}, or in the case of rocks from Mt. Amiata and Sabatini, Italy, by Fe^{2+} plus much subordinate Mn±Mg (Macdonald and Belkin, 2002). In a majority of our samples, there is not enough Fe to fill the site and, since Mn is not present in amounts sufficient to make up the difference, Mg is required in that role, to a maximum of 0.46 a.p.f.u. The chevkinite-group mineral from Mt. Riiser-Larsen, Napier Complex studied by Hokada (2007) is similarly Fe-depleted (0.5 a.p.f.u.), but the mineral from the Vestfold Hills has the lowest Fe content reported to date (0.05 a.p.f.u., Harley, 1994). This mineral is one of the two samples with an unfilled *B* site, (Mg = 0.78 and Mn = 0 a.p.f.u.), the other being a chevkinite from Khibina, Kola Peninsula (Yakovenchuk *et al*., 2005). However, if Zr and Hf were assumed to occupy *B* as Zr does in rengeite (Miyawaki *et al*., 2002), then the *B* occupancy would increase to 0.93 and 1.06 in the Vestfold Hills and Khibiny samples, respectively.

The C site

Cation sums in the *C* site are, with two exceptions, within 4% of the theoretical value of 2. The exceptions are samples 2234E (ΣC = 2.586) and 2275 (2.205). It may be no coincidence that these samples have, uniquely in our data set,

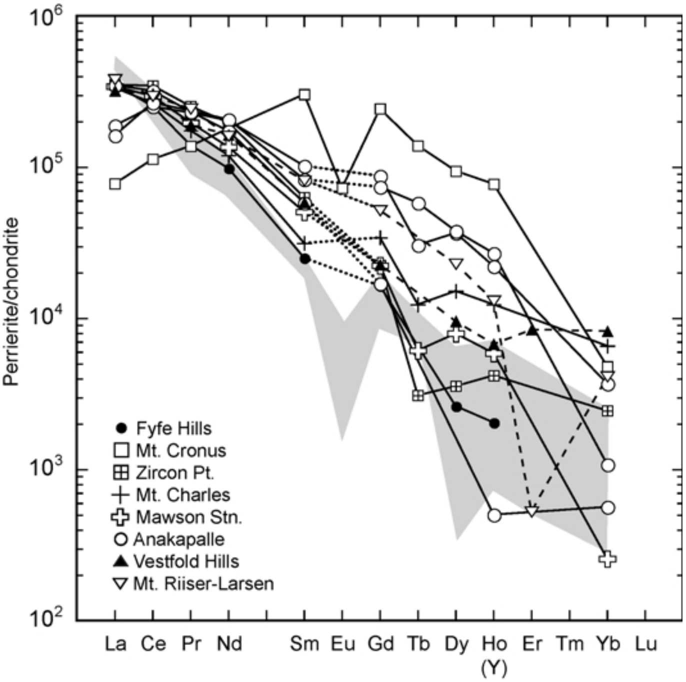

FIG. 6. Chondrite-normalized *REE* plots for selected chevkinite-group minerals from Antarctica and the Eastern Ghats, to demonstrate (1) the variability in patterns, and (2) the relative *MREE* and *HREE* enrichment compared to chevkinites and perrierites from the literature (as exemplified by the shaded field from Macdonald and Belkin, 2002). Yttrium is taken to proxy for Ho in the plot. Patterns dotted between Sm and Gd due to an absence of Eu data. Normalizing factors from Sun and McDonough (1989).

Ti abundances unable to fill the *D* site (1.434 and 1.788, respectively). This situation, unknown in normal chevkinite and perrierite (Macdonald and Belkin, 2002), raises the possibility that some Al may enter the *D* site. In fact, the *C* site excess is of a sufficient magnitude to compensate for the Ti (*D*) site deficiency.

Aluminium is the dominant cation in the *C* site, and would fill it in the case of samples 2234E and 2275 unless Al makes up the deficiency in the *D* site in these two samples. This is the strongest Al enrichment (up to 9.15 wt.% Al_2O_3) yet recorded in a chevkinite-group mineral and is in line with the reports by Harley (1994) and Hokada (2007) of large Al contents in the *C* sites of Antarctic perrierites.

The D site

With the exception of the two samples noted above, the *D* site is filled with Ti, and in all samples, Ti is the dominant cation at this site.

The tetrahedral site

Silicon ranges between 4 and 4.29 a.p.f.u., thus filling the tetrahedral site. The values >4 are probably due to minor analytical error.

Nomenclature

Given the site occupancies inferred above, none of the analysed samples is perrierite, if this mineral is understood to have dominantly Fe or Ti at the *C* site. Instead, because Al turns out to be the dominant cation at this site, the mineral from all the localities studied by us could be provisionally called the Al-dominant analogue of perrierite-(Ce), as is the mineral studied by Hokada (2007). The mineral from Mt. Cronus differs further in that Y is dominant among *REE* + Y, so it could be provisionally termed the Al-dominant analogue of perrierite-(Y).

However, this discussion leads to the question: which sites should be used to distinguish species within the chevkinite group? In recognizing dingdaohengite-(Ce) as distinct from chevkinite-(Ce), Xu *et al*. (2008) cited the *C* site as a criterion to distinguish this species within the chevkinite group. Applying this criterion, the Al-dominant analogue of perrierite-(Ce) is potentially a new species. Moreover, use of Levinson modifiers implies that the *A* site is also a criterion, and the Al-dominant analogue of perrierite-(Y) would thus become the second potentially new species among the samples reported here. Thirdly, the distinction between rengeite and matsubaraite implies that the *B* site has also been used as a criterion, and that the Mg-dominant Vestfold Hills mineral described by Harley (1994) is a third potentially new species, the Mg,Al-dominant analogue of perrierite-(Ce).

Table 1 lists end-member formulae for known and some potential species using the *A*, *B* and *C* sites as criteria to distinguish them; other combinations of *REE*, Ca, Sr, Zr, Fe^{2+}, Mg, Fe^{3+}, Cr and Ti could lead to a host of others, not to mention potential Y- and La-dominant end-members (the latter was reported by Segalstad and Larsen, 1978). Moreover, the three sites do not exhaust the possibilities; there are two *A* sites and the *D* site. While the latter is invariably dominated by Ti, the different *A* sites could differ in composition.

The recently described Fe-Ti-dominant chevkinite-subgroup minerals maoniupingite-(Ce) (IMA2003-017, Shen *et al*., 2005) and dingdaohengite-(Ce) (IMA 2005-14, Xu *et al*., 2008) were introduced without properly clarifying their relationship to chevkinite-(Ce). The formula calculated from the analysis of maoniupingite-(Ce) reported by Shen *et al*. (2005) can be expressed as a mixture of 61% $Ce_4Fe^{2+}(Fe^{3+}_2)Ti_2Si_4O_{22}$, 22% $Ca_4Ti(Ti_2)Ti_2Si_4O_{22}$ and minor amounts of other components, i.e. it is predominantly chevkinite-(Ce) as later defined for the purpose of distinguishing chevkinite-(Ce) from dingdaohengite-(Ce). The end-member formula $Ce_4Fe^{3+}(Fe^{3+}_2)Ti_2Si_4O_{22}$ that Xu *et al*. (2008) gave for maoniupingite-(Ce) does not correspond to the Shen *et al*. (2005) electron microprobe and Mössbauer spectroscopic analysis, which we calculate to yield 0.77 Fe^{2+}, 0.05 Mn and 0.05 Mg, almost sufficient to fill the *B* site. Moreover, the Xu *et al*. (2008) end-member formula is not balanced in charge.

Our end-member formula for dingdaohengite-(Ce), $Ce_4Fe^{2+}(Fe^{2+}Ti)Ti_2Si_4O_{22}$, differs from $Ce_4Fe^{2+}(Ti_2)Ti_2Si_4O_{22}$, the ideal end-member given by Xu *et al*. (2008). Their ideal formula is not charge-balanced, although their empirical formula with Ti dominant at the *C* site is. By invoking one of the characteristics of end-member formulae that Hawthorne (2002) recommended in defining new mineral species, *viz*. that an end-member may have more than one type of cation at one site 'if required by the electroneutrality principle', the formula given in Table 1 can be justified. In a chevkinite-group mineral with *REE* at the *A* site, this attribute of end-member formulae means that no more than 50% of the *C* site can be occupied by Ti unless its charge is balanced by a divalent cation at the site. As a result, our end-member composition does not meet the criterion of Ti dominance at the *C* site cited for distinguishing dingdaohengite-(Ce) from chevkinite-(Ce); the criterion would have to be Ti,Fe^{2+} instead.

Strontio-chevkinite is another problematic species. Miyawaki *et al*. (2002) re-indexed the XRD data of Haggerty and Mariano (1983) and suggested that strontio-chevkinite could be an Fe-rich variety of rengeite, i.e. in the perrierite subgroup. Our recalculation of the two chemical analyses reported by Haggerty and Mariano(1983) suggests that the rengeite end-member constitutes ~55% of strontio-chevkinite and its Ca analogue (Table 1) another 10%; a *REE*-Fe^{2+} end-member (Table 1) is one of the possible components making up the balance. In summary, the distinction between strontio-chevkinite and rengeite needs to be re-examined.

To resolve these issues, and the even more complicated problems in crystal structure which we have not broached here, it would be necessary to review systematically chevkinite-group nomenclature and explicitly lay out criteria and give charge-balanced end-members; only then could new species be defined in a proper manner. Such a review is best handled by a subcommittee of the Commission of New Minerals, Nomenclature and Classification, International Mineralogical Association (CNMNC IMA), and is clearly beyond the scope of the present paper.

Composition of chevkinite-group minerals, rock type and nature of protoliths

Macdonald and Belkin (2002) showed that perrierite has most commonly been recorded from mafic igneous rocks, such as anorthositic gabbro and pegmatite and K-rich volcanics of lamproitic or minette affinity, and from granodiorites and latites, where *REE*/Ca and Fe/Ca are normally low. Chevkinite and perrierite from different igneous parageneses were shown by Macdonald and Belkin (2002) to occupy discrete fields on a ($CaO+MgO+SrO+Al_2O_3$)-($\Sigma La_2O_3-Sm_2O_3$)-FeO* plot (Fig. 7). The Eastern Ghats and Antarctic data, including the analyses by Harley (1994) and Hokada (2007), plot roughly parallel to, but displaced to the Fe-poor side of, the field of perrierites from mafic and intermediate igneous rocks.

The analysed chevkinite-group minerals originated from three distinct parageneses, and their compositions reflect this. Samples 2131 and 2098A are from pegmatites containing hornblende and orthopyroxene or garnet intrusive into orthopyroxene-bearing quartzofelspathic rocks. These chevkinite-group minerals have relatively large FeO contents and small MgO and Al_2O_3 contents; their compositions plot in the field for mafic and intermediate igneous rocks (Fig. 7). Similarly, compositions of the chevkinite-group minerals in the orthopyroxene-bearing gneiss and granulite from Mt. Charles and the Fyfe Hills plot in this field. DePaolo *et al*. (1982) concluded that the protolith of sample 28-VII from the Fyfe Hills was a volcanic rock or a sediment consisting of immature detritus from an igneous terrane. A similar precursor is plausible for sample 2084E; i.e. these chevkinite-group minerals also did not crystallize in an aluminous environment. In contrast, the remaining samples, including that described by Hokada (2007), are highly aluminous paragneisses in which the associated minerals are relatively magnesian or aluminous: sapphirine, orthopyroxene, and sillimanite; even garnet has a relatively high Mg/Fe ratio: 55% pyrope and 43% almandine in 2234E (Grew *et al*., 2006). Chevkinite-group minerals in these samples are notably more aluminous and their Mg/Fe ratios greater than in the other samples analysed in this study. The Vestfold Hills chevkinite-group mineral represents an extreme in which the association in melt pools with sapphirine, spinel and enstatite approaching their

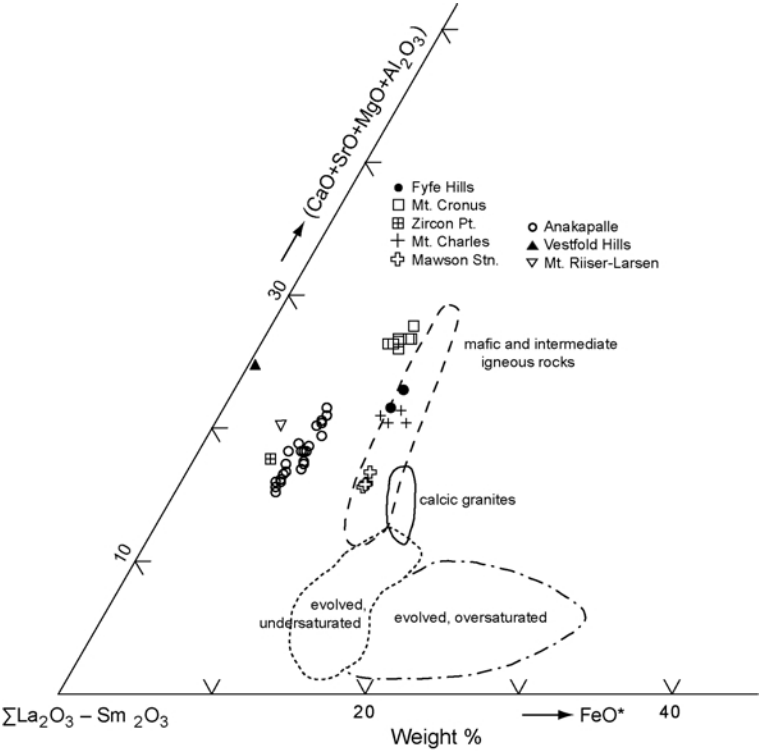

FIG. 7. Triangular plot showing the generalized fields of chevkinite and perrierite in various rock types (Macdonald and Belkin, 2002). The fields marked 'evolved, undersaturated' and 'evolved, oversaturated' are occupied only by chevkinite; the field of mafic and intermediate igneous rocks includes only perrierite. Both phases occur in the field of calcic granites.

respective Mg end-member compositions (Harley and Christy, 1995) results in a chevkinite-group mineral with 0.78 Mg and only 0.05 Fe at the *B* site (Harley, 1994), as well as an Al_2O_3 content as high as that in our chevkinite-group minerals from paragneiss. The aluminous chevkinite-group minerals with relatively high Mg/Fe ratio formed at temperatures possibly as high as 1000–1180ºC at pressures ranging from 3–4 kbar in the melt pools (Harley and Christy, 1995) to 7–10 kbar in the Napier Complex (e.g. Harley, 1998, 2008), conditions that extend the known stability range of the natural chevkinite-group minerals.

Acknowledgements

We thank G.E. Grikurov for sample 28-VII and Martin Yates for drawing our attention to the overlap of the Ce-$M\zeta$ and F-$K\alpha$ peaks. The Australian National Antarctic Research Expedition is thanked for logistics support of fieldwork during the 1977–1978 and 1979–1980 seasons, and the Indo-American Fellowship Program is thanked for support in India in 1980 and 1981. ESG's fieldwork in Antarctica was also supported by U.S. National Science Foundation grant DPP-7680957. We thank I-Ming Chou, Paul C. Hackley, Leonid Pautov, and Elena Sokolova for their helpful and constructive reviews. Any use of trade, product, or firm names is for descriptive purposes only and does not imply endorsement by the U.S. Government.

References

Asami, M., Suzuki, K., Grew, E.S. and Adachi, M. (1998) CHIME ages for granulites from the Napier complex, East Antarctica. *Polar Geoscience*, **11**, 172–199.

Asami, M., Suzuki, K. and Grew, E.S. (2002) Chemical Th-U-total Pb dating by electron microprobe analysis of monazite, xenotime and zircon from the Archean Napier complex, East Antarctica: evidence for ultra-high-temperature metamorphism at 2400 Ma. *Precambrian Research*, **114**, 249–275.

Atrashenok, L.Ya., Avdzeyko, G.V., Klimov, A.V., Krylov, A.Ya. and Silin, Yu.I. (1967) Comparative data on absolute ages of Antarctic rocks (lead and argon methods). *Akademiya Nauk SSSR Komissiya po Opredeleniyu Absolyutnogo Vozrasta Geologicheskikh Formatsii Trudy*, **14**, 227–229 (in Russian).

Bonatti, S. and Gottardi, G. (1966) Un caso di polimorfismo a strati in sorosilicati: perrierite chevkinite. *Periodico di Mineralogia*, **35**, 69–91.

Bose, S., Fukuoka, M., Sengupta, P. and Dasgupta, S. (2000) Evolution of high-Mg-Al granulites from Sunkarametta, Eastern Ghats, India: evidence for a lower crustal heating-cooling trajectory. *Journal of Metamorphic Geology*, **18**, 223–240.

Carlier, G. and Lorand, J.P. (2008) Zr-rich accessory minerals (titanite, perrierite, zirconolite, baddeleyite) record strong oxidation associated with magma mixing in the south Peruvian potassic province. *Lithos*, **104**, 54–70.

Crisp, R.S. (1991) Wavelengths of emission lines in the M spectrum of ^{49}In metal in the range of 12–265 AA. *Journal of Physics: Condensed Matter*, **3**, 927–932.

DePaolo, D.J., Manton, W.I., Grew, E.S. and Halpern, M. (1982) Sm-Nd, Rb-Sr and U-Th-Pb systematics of granulite facies rocks from Fyfe Hills, Enderby Land, Antarctica. *Nature*, **298**, 614–618.

Grew, E.S. (1982) Sapphirine, kornerupine, and sillimanite + orthopyroxene in the charnockitic region of South India. *Journal of the Geological Society of India*, **23**, 469–505.

Grew, E.S. (1998) Boron and beryllium minerals in granulite-facies pegmatites and implications of beryllium pegmatites for the origin and evolution of the Archean Napier Complex of East Antarctica. *Memoirs of the National Institute of Polar Research, Special Issue*, **53**, 74–92.

Grew, E.S. and Manton, W.I. (1979*a*) Archean rocks in Antarctica: 2.5-billion-year uranium-lead ages of pegmatites in Enderby Land. *Science*, **206**, 443–445.

Grew, E.S. and Manton, W.I. (1979*b*) Geochronologic studies in East Antarctica: Age of a pegmatite in Mawson charnockite. *Antarctic Journal of the United States*, **14 (5)**, 2–3.

Grew, E.S. and Manton, W.I. (1986) A new correlation of sapphirine granulites in the Indo-Antarctic metamorphic terrain: late Proterozoic dates from the Eastern Ghats Province of India. *Precambrian Research*, **33**, 123–137.

Grew, E.S., Yates, M.G., Barbier, J., Shearer, C.K., Sheraton, J.W., Shiraishi, K. and Motoyoshi, Y. (2000) Granulite-facies beryllium pegmatites in the Napier Complex in Khmara and Amundsen Bays, western Enderby Land, East Antarctica. *Polar Geoscience*, **13**, 1–40.

Grew, E.S., Yates, M.G., Shearer, C.K., Hagerty, J.J., Sheraton, J.W. and Sandiford, M. (2006) Beryllium and other trace elements in paragneisses and anatectic veins of the ultrahigh-temperature Napier Complex, Enderby Land, East Antarctica: the role of sapphirine. *Journal of Petrology*, **47**, 859–882.

Grew, E.S., Hålenius, U. Pasero, M. and Barbier, J. (2008) Recommended nomenclature for the sapphirine and surinamite groups (sapphirine supergroup). *Mineralogical Magazine*, **72**, 839–876.

Haggerty, S.E. and Mariano, A.N. (1983) Strontian-loparite and strontio-chevkinite: Two new minerals in rheomorphic fenites from the Paraná Basin carbonatites, South America. *Contributions to Mineralogy and Petrology*, **84**, 365–381.

Halpin, J.A., Gerakiteys, C.L., Clarke, G.L., Belousova, E.A. and Griffin, W.L. (2005) In-situ U-Pb geochronology and Hf isotope analyses of the Rayner Complex, east Antarctica. *Contributions to Mineralogy and Petrology*, **148**, 689–706.

Harley, S.L. (1994) Mg-Al yttrian zirconolite in a partially melted sapphirine granulite, Vestfold Hills, East Antarctica. *Mineralogical Magazine*, **58**, 259–269.

Harley, S. (1998) On the occurrence and characterization of ultrahigh-temperature crustal metamorphism. Pp. 81–107 in: *What Drives Metamorphism and Metamorphic Reactions?* (P.J. Treloar and P.J. O'Brien, editors). Special Publications, **138,** The Geological Society, London.

Harley, S. (2008) Refining the *P-T* records of UHT crustal metamorphism. *Journal of Metamorphic Geology*, **26**, 125–154.

Harley, S.L. and Christy, A.G. (1995) Titanium-bearing sapphirine in a partially melted aluminous granulite xenolith, Vestfold Hills, Antarctica: geological and mineralogical implications. *European Journal of Mineralogy*, **7**, 637–653.

Hawthorne, F.C. (2002) The use of end-member charge-arrangements in defining new mineral species and heterovalent substitutions in complex minerals. *The Canadian Mineralogist*, **40**, 699–710.

Hokada, T. (2007) Perrierite in sapphirine–quartz gneiss: geochemical and geochronological features and implications for accessory-phase paragenesis of UHT metamorphism. *Journal of Mineralogical and Petrological Sciences*, **102**, 44–49.

Johnson, G.G., Jr. and White, E.W. (1970) *X-ray Emission Wavelengths and keV Tables for Nondestructive Analysis*. American Society for Testing and Materials Data Series DS 46, Philadelphia, Pennsylvania, USA.

Kamenev, Ye.N. (1972) Geological structure of Enderby Land. Pp. 579–583 in: *Antarctic Geology and Geophysics* (R.J. Adie, editor). Universitetsforlaget, Oslo.

Lima-de-Faria, J. (1962) Heat treatment of chevkinite and perrierite. *Mineralogical Magazine*, **33**, 42–47.

Macdonald, R. and Belkin, H.E. (2002) Compositional variation in minerals of the chevkinite group. *Mineralogical Magazine*, **66**, 1075–1098.

Miyawaki, R., Matsubara, S. and Miyajima, H. (2002) The crystal structure of rengeite, $Sr_4ZrTi_4(Si_2O_7)_2O_8$. *Journal of Mineralogical and Petrological Sciences*, **97**, 7–12.

Parodi, G.C., Della Ventura, G., Montana, A. and Raudsepp, M. (1994) Zr-rich non metamict perrierite-(Ce) from holocrystalline ejecta in the Sabatini volcanic complex (Latium, Italy). *Mineralogical Magazine*, **58**, 607–613.

Sarkar, S., Dasgupta, S. and Fukuoka, M. (2003) Petrological evolution of a suite of spinel granulites from Vizianagram, Eastern Ghats Belt, India, and genesis of sapphirine-bearing assemblages. *Journal of Metamorphic Geology*, **21**, 899–913.

Segalstad, T.V. and Larsen, A.O. (1978) Chevkinite and perrierite from the Oslo region, Norway *American Mineralogist*, **63**, 499–505.

Sengupta, P., Sen, J., Dasgupta, S., Raith, M., Bhui, U.K. and Ehl, J. (1999) Ultra-high temperature metamorphism of metapelitic granulites from Kondapalle, Eastern Ghats Belt: Implications for the Indo-Antarctic correlation. *Journal of Petrology*, **40**, 1065–1087.

Shen, G., Yang, G. and Xu, J. (2005) Maoniupingite-(Ce): a new rare-earth mineral from the Maoniuping rare-earth deposit in Mianning, Sichuan. *Sedimentary Geology and Tethyan Geology (Chenji yu Tetisi Dizhi)*, **25**, 210–216 [in Chinese with English abstract].

Sheraton, J.W. (1982) Origin of charnockitic rocks of MacRobertson Land. Pp. 489–497 in: *Antarctic Geoscience* (C. Craddock, editor). University of Wisconsin Press, Madison, USA.

Sheraton, J.W., Tingey, R.J., Black, L.P, Offe, L.A. and Ellis, D.J. (1987) Geology of an unusual Precambrian high-grade metamorphic terrane – Enderby Land and western Kemp Land, Antarctica. *Department of Resources and Energy, Bureau of Mineral Resources, Geology and Geophysics Bulletin*, **223**, 1–51.

Shimazaki, H., Yang, Z., Miyawaki, R. and Shigeoka, M. (2008) Scandium-bearing minerals in the Bayan Obo Nb-REE-Fe deposit, Inner Mongolia, China. *Resource Geology*, **58**, 80–86.

Sokolova, E., Hawthorne, F.C., Della Ventura, G. and Kartashov, P.M. (2004) Chevkinite-(Ce): crystal structure and the effect of moderate radiation-induced damage on site-occupancy refinement. *The Canadian Mineralogist*, **42**, 1013–1025.

Song, R., Ding, K. and Li, Z. (1999) Site occupancies of iron in saimaite and chevkinite. *Chinese Science Bulletin*, **44**, 2274–2276.

Sun, S-S. and McDonough, W.F. (1989) Chemical and isotopic systematics of oceanic basalts: implications for mantle composition and processes. Pp. 313–345 in: *Magmatism in the Ocean Basins* (A.D. Saunders and M.J. Norry, editors). Special Publications, **42**, The Geological Society, London.

van Bergen, M.J. (1984) Perrierite in siliceous lavas from Mt Amiata, central Italy. *Mineralogical*

Magazine, **48**, 553–556.

Wendt, M. and Christ, B. (1985) The relative intensity of Mζ-lines. *Crystal Research and Technology*, **20**, 1443–1449.

Xu, J., Yang, G., Li, G., Wu, Z. and Shen, G. (2008) Dingdaohengite-(Ce) from the Bayan Obo REE-Nb-Fe Mine, China: Both a true polymorph of perrierite-(Ce) and a titanic analog at the *C*1 site of chevkinite subgroup. *American Mineralogist*, **93**, 740–744.

Yakovenchuk, V.N., Ivanyuk, G.Yu., Pakhomovsky, Ya.A. and Menshikov, Yu.P. (2005) *Khibiny*. (F. Wall, editor). Laplandia Minerals, Apatity, in association with the Mineralogical Society of Great Ireland and Ireland, 448 pp.

Young, D.N. and Black, L.P. (1991) U-Pb zircon dating of Proterozoic igneous charnockites from the Mawson Coast, East Antarctica. *Antarctic Science*, **3**, 205–216.

Young, D.N., Zhao, J.-X., Ellis, D.J. and McCulloch, M.T. (1997) Geochemical and Sr-Nd isotopic mapping of source provinces for the Mawson charnockites, East Antarctica: implications for Proterozoic tectonics and Gondwana reconstruction. *Precambrian Research*, **86**, 1–19.